

Scattering of Polarized μ Mesons from Extended Nuclei*

GEORGE H. RAWITSCHER†

Department of Physics and Astronomy, University of Rochester, Rochester, New York

(Received July 31, 1958)

Scattering solutions of the Dirac equation for a muon in the static electric field of an extended nucleus are numerically obtained for various values of the velocity of the incident particle ($\beta=0.4$ to 0.8) and of the charge of the scattering nucleus ($Z=48$ and 80). A Stanford Fermi-type shape for the extended nuclear charge distribution is assumed. Angular distributions of the unpolarized cross section and of the left-right scattering asymmetries (S) of a transversely polarized beam of μ^+ and μ^- mesons are presented. For μ^- the finite nuclear size strongly reduces S in the forward directions. The reduction of the cross section seems to be more sensitive to the detailed shape of the charge distribution than is the reduction of S . In the case of μ^+ , S is appreciably altered from the "point" value, and can depend sensitively on the shape of the nuclear charge distribution. The value of S can be larger for the extended nucleus than for the point nucleus.

INTRODUCTION

MEASUREMENT of the polarization of spin- $\frac{1}{2}$ particles emitted in weak interaction decay has recently become of importance. In particular, muons arising from pion decay are known¹ to be polarized because of their decay asymmetries, but the magnitude and sign of the polarization has as yet not been meas-

TABLE I. μ^- ; $\beta=0.6$; $Z=48, 80, 92$. Percent polarization^a $100 S$ and differential cross section σ (in 10^{-26} cm² per sterad) for negative muons of 26.42 Mev kinetic energy incident on the extended nuclei of Cd, Hg, and U. The shape of the nuclear charge distribution used is given in Eq. (1) of the text. The scattering angle θ is in degrees.

θ		$Z=48$	$Z=80$	$Z=92$
30°	100 S	-0.376	-0.552	-0.602
	σ	99.7	320.1	451.4
45°	100 S	-0.952	-1.612	-1.79
	σ	12.4	34.6	47.7
60°	100 S	-1.58	-3.4	-3.47
	σ	1.96	4.64	6.42
75°	100 S	-2.56	-5.33	-5.32
	σ	0.331	0.857	1.26
90°	100 S	-5.19	-6.70	-6.14
	σ	0.0642	0.244	0.348
105°	100 S	-10.0	-6.32	-5.91
	σ	0.0196	0.0834	0.101
120°	100 S	-13.0	-5.56	-6.45
	σ	0.0101	0.0274	0.0280
135°	100 S	-13.3	-9.48	-15.05
	σ	6.40×10^{-3}	8.72×10^{-3}	9.10×10^{-3}
150°	100 S	-11.7	-24.02	-30.59
	σ	4.37×10^{-3}	3.56×10^{-3}	5.12×10^{-3}
165°	100 S	-7.22	-24.08	-24.43
	σ	3.34×10^{-3}	2.56×10^{-3}	4.59×10^{-3}

^a See reference 2.

* Work supported in part by the U. S. Atomic Energy Commission.

† Now at Physics Department, Yale University, New Haven, Connecticut.

¹ Garwin, Lederman, and Weinrich, Phys. Rev. **105**, 1415 (1957).

ured. The experimental difficulty lies in the smallness of the spin-dependent effects. Neither Møller scattering nor bremsstrahlung, which permit the measurement of electron polarization, are suitable in the case of the muon. Therefore, it is worth while to investigate the Mott scattering of muons polarized transversely to the direction of motion, although the left-right scattering asymmetries result to be of the order of 20% or less.

Some theoretical curves for the scattering cross section and polarization² of μ^- mesons on extended

TABLE II. μ^+ ; $\beta=0.4$; $Z=48, 80, 92$. Same as Table I for positive muons of 9.63 Mev kinetic energy.

θ		$Z=48$	$Z=80$	$Z=92$
30°	100 S	0.201	0.158	0.148
	σ	758	2.10×10^3	2.78×10^3
45°	100 S	0.358	0.281	0.253
	σ	155	433	563.0
60°	100 S	0.484	0.378	0.338
	σ	51.7	146	193.8
75°	100 S	0.560	0.438	0.392
	σ	22.8	65.6	86.9
90°	100 S	0.581	0.457	0.410
	σ	12.1	35.5	47.1
105°	100 S	0.553	0.437	0.394
	σ	7.43	22.1	29.4
120°	100 S	0.484	0.389	0.352
	σ	5.10	15.4	20.5
135°	100 S	0.383	0.315	0.285
	σ	3.86	11.7	15.7
150°	100 S	0.267	0.221	0.198
	σ	3.18	9.77	13.0
165°	100 S	0.140	0.117	0.101
	σ	2.84	8.77	11.7

² The word "polarization" is used henceforth to denote the polarization of an initially unpolarized beam scattered through an angle θ . The definition of the function $S(\theta)$ adopted here is the same as that given in reference 3, Eqs. (5) to (8). In this reference the connection between $S(\theta)$ and the left-right scattering asymmetry of an incident polarized beam is reviewed. For example, in the case of an incident beam polarized transversely in the "up"

nuclei have become available recently.³ These calculations consist in modifying the point Coulomb wave function given by Sherman⁴ in order to take into account the finite nuclear size. The results show that the effect of the nuclear extension is to reduce greatly the polarization from the point Coulomb values in the forward directions, which is just where the cross sections are largest. The above-mentioned calculations are limited to velocities $v/c \leq 0.4$ and use a uniform charge distribution for the nucleus.

The results presented in this paper complement those of reference 3 by including the case of positive muons, by extending the velocity to $v/c=0.8$, and by using the more realistic "Fermi shape" for the nuclear charge distribution as fitted to the Stanford electron scattering experiments.⁵

TABLE III. μ^+ ; $\beta=0.6$; $Z=48, 80, 92$. Same as Table I for positive muons of 26.42 Mev kinetic energy.

θ		$Z=48$	$Z=80$	$Z=92$
30°	100 S	0.281	0.388	0.420
	σ	103	306	410
45°	100 S	0.335	0.464	0.530
	σ	18.2	57.9	79.2
60°	100 S	0.212	0.317	0.405
	σ	5.03	17.2	24.1
75°	100 S	-0.109	0.00	0.104
	σ	1.80	6.61	9.50
90°	100 S	-0.572	-0.406	-0.279
	σ	0.769	3.05	4.49
105°	100 S	-1.05	-0.778	-0.638
	σ	0.381	1.63	2.45
120°	100 S	-1.41	-1.02	-0.881
	σ	0.215	0.983	1.51
135°	100 S	-1.51	-1.06	-0.938
	σ	0.138	0.666	1.04
150°	100 S	-1.27	-0.877	-0.781
	σ	0.100	0.504	0.796
165°	100 S	-0.732	-0.490	-0.442
	σ	8.27×10^{-2}	0.427	0.679

An additional motivation for the present work was to provide reliable elastic cross sections with which experiments could be compared. The so called "anomalous scattering," found some time ago⁶ for muons of cosmic-

direction, the scattering cross section to the "left" (L) and that to the "right" (R) are related to S by $(L-R)/(L+R)=S(\theta)$.

³ J. Franklin and B. Margolis, Phys. Rev. **109**, 525 (1958).

⁴ N. Sherman, Phys. Rev. **103**, 1601 (1956).

⁵ R. Hofstadter, *Annual Review of Nuclear Science* (Annual Reviews, Inc., Stanford, 1957), Vol. 7, p. 231.

⁶ J. L. Lloyd and A. W. Wolfendale, Proc. Phys. Soc. (London) **A68**, 1045 (1955); I. B. McDiarmid, Phil. Mag. **46**, 1777 (1955); A. I. Alikhanov and G. P. Eliseev, Bull. acad. sci. U.R.S.S., Phys. Sér. **19**, 732 (1955) [Columbia Tech. Transl. **19**, 662 (1955)]; A. I. Alikhanov and V. G. Kirillov-Ugriumov, Bull. acad. sci. U.R.S.S., Phys. Sér. **19**, 737 (1955) [Columbia Tech. Transl. **19**, 667 (1955)]; S. Fukui *et al.*, Progr. Theoret. Phys. Japan **19**, 348 (1958); B. G. Chidley *et al.*, Can. J. Phys. **36**, 801 (1958).

TABLE IV. μ^+ ; $\beta=0.8$; $Z=48, 80$. Same as for Table I for positive muons of 70.47 Mev kinetic energy.

θ		$Z=48$	$Z=80$
30°	100 S	-0.06	-0.339
	σ	10.3	30.5
45°	100 S	-0.872	-1.61
	σ	0.891	2.52
60°	100 S	-2.67	-3.75
	σ	9.29×10^{-2}	0.262
75°	100 S	-5.88	-5.23
	σ	9.95×10^{-3}	3.13×10^{-2}
90°	100 S	-7.44	-2.59
	σ	1.21×10^{-3}	4.92×10^{-3}
105°	100 S	+0.07	+0.564
	σ	2.89×10^{-4}	1.22×10^{-3}
120°	100 S	+3.83	-2.35
	σ	1.41×10^{-4}	4.38×10^{-4}
135°	100 S	+2.03	-3.61
	σ	8.45×10^{-5}	1.87×10^{-4}
150°	100 S	-0.709	-0.668
	σ	5.52×10^{-5}	9.04×10^{-5}
165°	100 S	-0.567	+0.868
	σ	4.10×10^{-5}	5.44×10^{-5}

ray origin is still on uncertain footing. At present no real evidence exists for a μ -nuclear scattering interaction⁷ other than Coulomb.

TABLE V. μ^+ ; $\beta=0.8$; $Z=48, Z=80$; uniform. Same as Table IV but using a uniform nuclear charge distribution of the same rms radii as those of the Fermi shape used for the nuclei of Table IV.

θ		$Z=48$	$Z=80$
30°	100 S	-0.112	-0.365
	σ	10.3	29.9
45°	100 S	-0.920	-1.76
	σ	0.86	2.33
60°	100 S	-3.06	-4.06
	σ	7.98×10^{-2}	0.221
75°	100 S	-6.07	-4.09
	σ	7.33×10^{-3}	2.75×10^{-2}
90°	100 S	-1.43	-0.551
	σ	1.46×10^{-3}	6.14×10^{-3}
105°	100 S	3.28	-1.69
	σ	7.71×10^{-4}	1.99×10^{-3}
120°	100 S	0.736	-7.32
	σ	4.23×10^{-4}	6.58×10^{-4}
135°	100 S	-2.64	-14.5
	σ	2.18×10^{-4}	2.07×10^{-4}
150°	100 S	-4.63	-19.6
	σ	1.17×10^{-4}	6.70×10^{-5}
165°	100 S	-3.42	-14.7
	σ	7.47×10^{-5}	2.81×10^{-5}

⁷ I. B. McDiarmid, Phys. Rev. **109**, 1792 (1958).

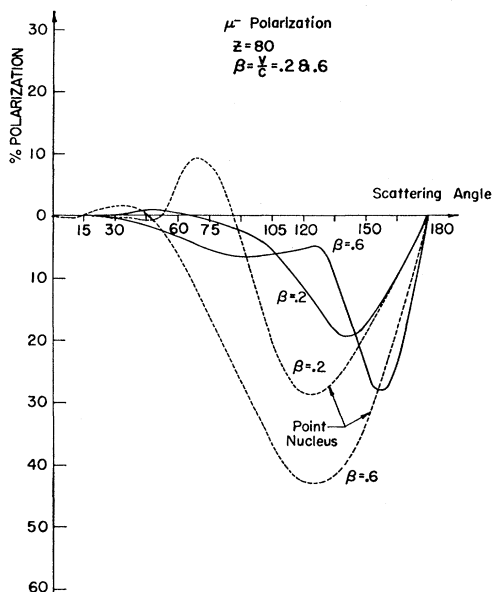


FIG. 1. The percent polarization² for μ^- scattering in the Coulomb field of an extended Hg nucleus for several velocities of the muon. The nuclear charge distribution is taken to be of the Fermi shape fitted to electron scattering at Stanford University [Eq. (1), text; $c_0 = 1.08 \times 10^{-13}$ cm; $t = 2.4 \times 10^{-13}$ cm]. The dashed curves, shown for comparison, refer to the point nucleus.

Our polarization and cross-section results are presented in Tables I to V and are illustrated in Figs. 1-5. The sensitivity of the polarization to the charge distribution is displayed in Figs. 6 and 7. The next section outlines the calculation method, and in the appendix some of the more useful formulas are transcribed.

CALCULATION

The Dirac equation is used to determine the scattered wave function. The solution is obtained in terms of the

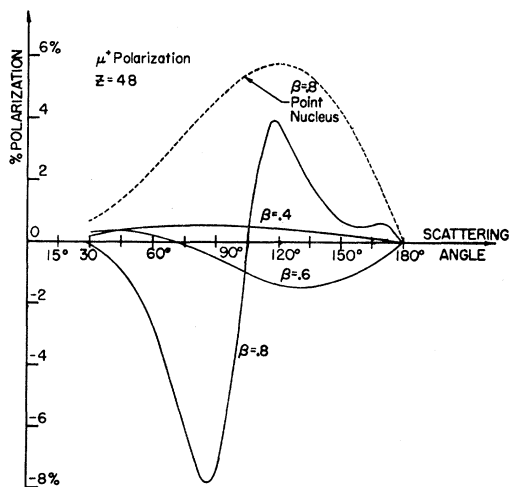


FIG. 2. Same as Fig. 1 referring now to positive muons scattering on Cd nuclei. Note that for $\beta = 0.8$, the polarization for the extended nucleus is larger than for the point nucleus.

well-known⁸ method of partial wave expansion. The potential acting on the muon is assumed to be entirely the result of static Coulomb interaction arising from a charge distribution $\rho(r)$ of the "Fermi shape"⁹:

$$\rho(r) = \rho_0 \{1 + \exp[(r-c)/z]\}^{-1} \quad \text{if } r < r_0, \quad (1a)$$

$$= 0 \quad \text{if } r \geq r_0, \quad (1b)$$

$$4\pi \int_0^\infty \rho(r)r^2 dr = Ze, \quad c = c_0 \times A^{1/3}, \quad z = t/4.4. \quad (1c)$$

Here r is the radial distance from the center of the nucleus, Ze and A are respectively the nuclear charge

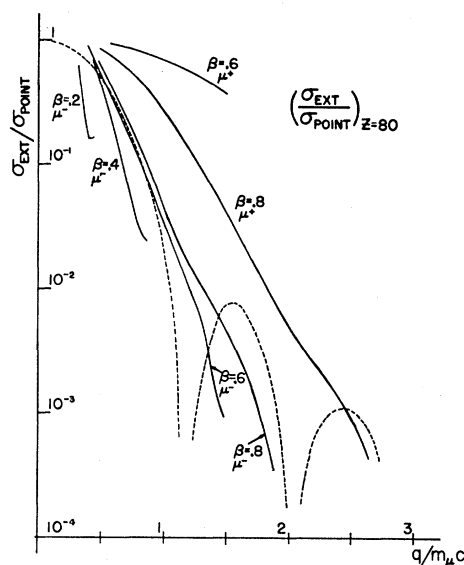


FIG. 3. The ratio of the differential cross sections for muon scattering on the extended Hg nucleus of the Fermi shape to that for a point nucleus. The momentum transfer is in units of $m_\mu c = 105.7$ Mev/ c and is given by the expression $q/m_\mu c = 2(p/m_\mu c) \sin(\theta/2)$, where p is the muon's incident momentum and θ the scattering angle. The dashed curve, shown in order to provide a comparison with older estimates, represents the ratio calculated in Born approximation for a uniform nuclear charge distribution of radius $R = 1.20 \times A^{1/3} \times 10^{-13}$ cm (where A is here 200). Again $\beta = v/c$. The author is indebted to Brown *et al.*¹⁴ for permission to use their $\beta = 0.8$ μ^- cross section result.

and the atomic number. The quantities c and t are the half-point radius and skin thickness, respectively, as defined in reference 9. In all the results denoted by the subscript "EXT," c_0 and t are taken,⁹ respectively, as 1.08×10^{-13} cm and 2.4×10^{-13} cm. The matching radius r_0 is determined so that less than 10^{-3} part of the nuclear charge would lie outside r_0 if the form (1a) for $\rho(r)$ were used from 0 to ∞ .

The scattering wave function is decomposed into a series of eigenfunctions of the angular momentum oper-

⁸ N. F. Mott and H. S. W. Massey, *The Theory of Atomic Collisions* (Clarendon Press, Oxford, 1949), second edition, Chap. 4, Sec. 4.

⁹ See reference 5, Eqs. (192), (193), and (194).

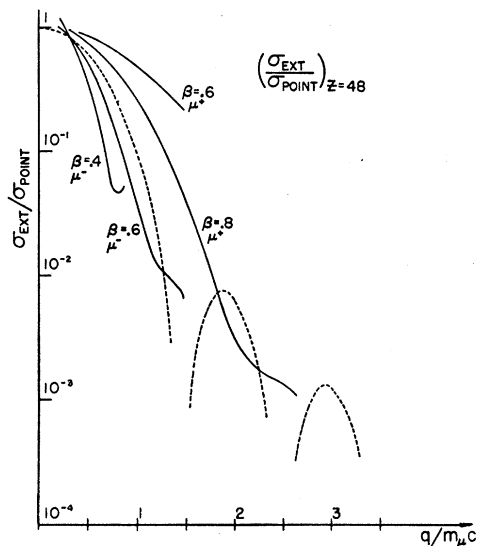


FIG. 4. Same as Fig. 3, referring now to muon scattering on Cd.

ator¹⁰ k , and the radius-dependent coefficients F_k and G_k are determined from the well known radial equations which they obey [appendix, Eq. (2A)]. The asymptotic behavior of the F 's and G 's determines the phase shifts η_k , from which $f(\theta)$ and $g(\theta)$ [see Eq. (15A)] and finally the cross section and polarization are calculated.

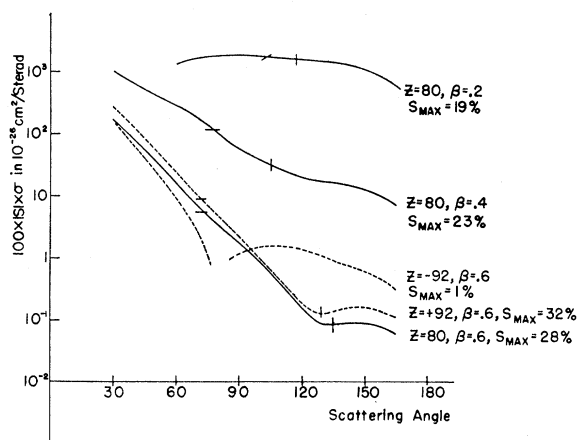


FIG. 5. The product of cross section and percent polarization² for negative muon scattering on the extended nucleus of Hg. The cross sections are in units of 10^{-28} cm² per steradian and $\beta = v/c$. To the left of the horizontal marks the polarization is less than 5%, to the left of the vertical marks it is less than 10%. The maximum polarization is indicated in each case. For comparison, the dashed curves are for μ^\pm scattering on uranium at $\beta = 0.6$. Notice that, although the polarization is small for $Z = -92$ (i.e., μ^+ scattering), the cross section is so large as to raise the values of the product above the $Z = 92$ curve, beyond 100° .

¹⁰ L. I. Schiff, *Quantum Mechanics* (McGraw-Hill Book Company, Inc., New York, 1949), Eq. (44.10). The eigenvalues of k are the integers $\pm 1, \pm 2, \dots$ etc., also denoted by the letter k . For $k = +|k|$ the orbital angular momentum l of the partial wave is equal to $k - 1$, and for $k = -|k|$, $l = |k|$. In both cases the total angular momentum j is equal to $|k| - \frac{1}{2}$.

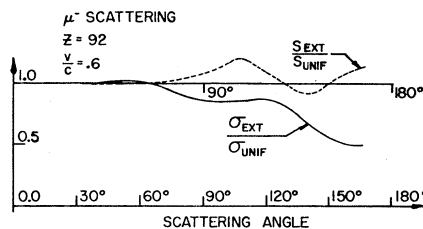


FIG. 6. The sensitivity of the polarization² S and the cross section σ to the detailed nuclear shape at $\beta = 0.6$ on uranium. The subscript EXT refers to a Fermi-type nuclear shape defined in Eq. (1), text, with the parameters c_0 and l taken equal respectively to 1.08 and 2.4 times 10^{-13} cm. The subscript UNIF refers to a uniform nuclear charge distribution with a radius so chosen that the rms radii for the EXT and UNIF shapes are the same.

The evaluation of the η_k occurs in much the same way as in the work of Yennie *et al.*,¹¹ by means of numerically integrating the radial Eqs. (2A) up to r_0 and there matching the results to a combination of the regular and irregular point Coulomb solutions $F_k^R, F_k^I, G_k^R, G_k^I$. The major difference of the present calculation from that of reference 11 lies in the fact that the rest mass of the muon cannot be neglected in comparison to the total energy, and therefore $\eta_{|k|}$ is no longer equal to $\eta_{-|k|}$. Thus, two phase shifts are required here for each value of $|k|$.

As k increases the phase shifts approach the point Coulomb phase shifts η_k^c . When the difference becomes less than 10^{-4} , the η_k^c are substituted directly for the η_k , and the calculation proceeds until the third-order reduced¹² coefficients of the Legendre polynomials required in the sum of $f(\theta)$ and $g(\theta)$ have a value less than

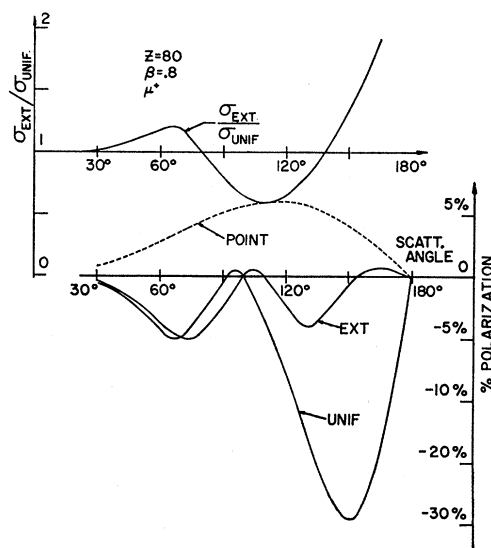


FIG. 7. Same as in Fig. 6, now referring to positive muons scattering on Hg nuclei with velocity $\beta = 0.8$. The % polarization for the extended and uniform nuclei are plotted separately (lower part of figure), rather than their ratio.

¹¹ Yennie, Ravenhall, and Wilson, *Phys. Rev.* **95**, 500 (1954).

¹² Defined in reference 11, Eqs. (47) to (49).

TABLE VI. μ^+ ; $\beta=0.4$; $Z=48, 80, 92$; point. Percent polarization^a $100 S_0$ and differential cross section σ_0 (in units of 10^{-26} cm² per sterad) for positive muons of 9.63 Mev kinetic energy scattering on the point nuclei of Cd, Hg, and U. The quantities f and g are defined in Eqs. (15A) and (17A).

θ		Z=48	Z=80	Z=92
30°	Re f	6.23	39.7	12.0
	Im f	-26.7	22.9	51.3
	Re g	0.125	0.592	0.147
	Im g	-0.417	0.383	0.795
	$100 S_0$	+0.199	0.155	0.146
	σ_0	755	2.10×10^3	2.78×10^3
45°	Re f	-5.28	17.3	23.9
	Im f	-11.3	-11.5	1.56
	Re g	-8.41×10^{-2}	0.346	0.450
	Im g	-0.236	-0.195	5.94×10^{-2}
	$100 S_0$	0.382	0.278	0.249
	σ_0	155	432	572
60°	Re f	-5.63	2.78	9.68
	Im f	-4.55	-11.8	-9.99
	Re g	-0.112	8.06×10^{-2}	0.217
	Im g	-0.116	-0.239	-0.189
	$100 S_0$	0.559	0.388	0.342
	σ_0	52.5	146	194
75°	Re f	-4.56	-2.55	1.26
	Im f	-1.65	-7.69	-9.24
	Re g	-9.70×10^{-2}	-3.53×10^{-2}	4.50×10^{-2}
	Im g	-5.33×10^{-2}	-0.167	-0.189
	$100 S_0$	0.702	0.467	0.407
	σ_0	23.6	65.7	87.0
90°	Re f	-3.56	-4.02	-2.32
	Im f	-0.340	-4.42	-6.47
	Re g	-7.54×10^{-2}	-6.84×10^{-2}	-3.14×10^{-2}
	Im g	-2.14×10^{-2}	-9.77×10^{-2}	-0.132
	$100 S_0$	0.788	0.504	0.436
	σ_0	12.8	35.7	47.3
105°	Re f	-2.81	-4.12	-3.55
	Im f	0.277	-2.32	-4.11
	Re g	-5.59×10^{-2}	-6.73×10^{-2}	-5.36×10^{-2}
	Im g	-5.94×10^{-3}	-5.13×10^{-2}	-7.98×10^{-2}
	$100 S_0$	0.806	0.497	0.427
	σ_0	7.99	22.3	29.5
120°	Re f	-2.29	-3.81	-3.81
	Im f	+0.573	-1.05	-2.48
	Re g	-4.00×10^{-2}	-5.45×10^{-2}	-5.15×10^{-2}
	Im g	8.67×10^{-4}	-2.43×10^{-2}	-4.41×10^{-2}
	$100 S_0$	0.752	0.451	0.387
	σ_0	5.58	15.6	20.7
135°	Re f	-1.94	-3.45	-3.71
	Im f	0.717	-0.309	-1.45
	Re g	-2.73×10^{-2}	-3.95×10^{-2}	-4.04×10^{-2}
	Im g	3.17×10^{-3}	-1.00×10^{-2}	-2.25×10^{-2}
	$100 S_0$	0.629	0.372	0.316
	σ_0	4.28	12.0	15.9
150°	Re f	-1.72	-3.16	-3.54
	Im f	0.785	0.107	-0.830
	Re g	-1.70×10^{-2}	-2.53×10^{-2}	-2.70×10^{-2}
	Im g	3.04×10^{-3}	-3.31×10^{-3}	-1.04×10^{-2}
	$100 S_0$	0.455	0.264	0.221
	σ_0	3.56	9.98	13.2
165°	Re f	-1.59	-2.98	-3.41
	Im f	0.814	0.317	-0.506
	Re g	-8.13×10^{-3}	-1.22×10^{-2}	-1.33×10^{-2}
	Im g	1.74×10^{-3}	-7.93×10^{-4}	-3.94×10^{-3}
	$100 S_0$	0.240	0.139	0.113
	σ_0	3.20	8.97	11.9

^a See reference 2.

TABLE VII. μ^+ ; $\beta=0.6$; $Z=48, 80, 92$; point. Same as Table VI for positive muons of 26.42 Mev kinetic energy.

θ		Z=48	Z=80	Z=92
30°	Re f	-4.66	9.92	17.1
	Im f	-9.31	-14.7	-10.4
	Re g	-0.172	+0.390	0.693
	Im g	-0.398	-0.493	-0.371
	$100 S_0$	0.461	0.528	0.426
	σ_0	108	314	400
45°	Re f	-3.64	-1.14	1.83
	Im f	-2.91	-7.70	-8.77
	Re g	-0.186	-2.01×10^{-2}	0.129
	Im g	-0.177	-0.401	-0.433
	$100 S_0$	0.938	0.996	0.843
	σ_0	21.8	60.7	80.4
60°	Re f	-2.48	-2.60	-1.74
	Im f	-1.00	-3.63	-4.84
	Re g	-0.150	-0.124	-6.70×10^{-2}
	Im g	-8.22×10^{-2}	-0.226	-0.283
	$100 S_0$	1.49	1.34	1.27
	σ_0	7.18	20.0	26.6
75°	Re f	-1.74	-2.44	-2.32
	Im f	-0.301	-1.67	-2.50
	Re g	-0.114	-0.130	-0.113
	Im g	-3.79×10^{-2}	-0.121	-0.164
	$100 S_0$	2.02	1.77	1.64
	σ_0	3.14	8.80	11.7
90°	Re f	-1.29	-2.04	-2.16
	Im f	-1.18×10^{-2}	-0.711	-1.24
	Re g	-8.60×10^{-2}	-0.109	-0.108
	Im g	-1.64×10^{-2}	-6.18×10^{-2}	-8.93×10^{-2}
	$100 S_0$	2.42	2.06	1.89
	σ_0	1.66	4.68	6.22
105°	Re f	-0.997	-1.68	-1.87
	Im f	0.116	-0.225	-0.558
	Re g	-6.40×10^{-2}	-8.53×10^{-2}	-8.89×10^{-2}
	Im g	-5.93×10^{-3}	-2.99×10^{-2}	-4.66×10^{-2}
	$100 S_0$	2.63	2.16	1.97
	σ_0	1.01	2.87	3.82
120°	Re f	-0.812	-1.40	-1.61
	Im f	+0.174	2.92×10^{-2}	-0.185
	Re g	-4.66×10^{-2}	-6.30×10^{-2}	-6.74×10^{-2}
	Im g	-1.01×10^{-3}	-1.32×10^{-2}	-2.30×10^{-2}
	$100 S_0$	2.68	2.07	1.86
	σ_0	0.692	1.98	2.63
135°	Re f	-0.692	-1.21	-1.41
	Im f	0.201	0.164	$+2.16 \times 10^{-2}$
	Re g	-3.25×10^{-2}	-4.40×10^{-2}	-4.77×10^{-2}
	Im g	9.37×10^{-4}	-4.96×10^{-3}	-1.05×10^{-2}
	$100 S_0$	2.26	1.77	1.58
	σ_0	0.521	1.50	2.00
150°	Re f	-0.618	-1.09	-1.28
	Im f	0.213	0.234	+0.134
	Re g	-2.06×10^{-2}	-2.78×10^{-2}	-3.02×10^{-2}
	Im g	1.29×10^{-3}	-1.33×10^{-3}	-4.25×10^{-3}
	$100 S_0$	1.68	1.29	1.15
	σ_0	0.428	1.24	1.65
165°	Re f	-0.578	-1.02	-1.20
	Im f	0.218	0.268	+0.189
	Re g	-1.00×10^{-2}	-1.34×10^{-2}	-0.146×10^{-2}
	Im g	8.27×10^{-4}	-1.42×10^{-4}	-1.40×10^{-3}
	$100 S_0$	0.892	0.677	0.603
	σ_0	0.381	1.11	1.48

10^{-4} . This procedure, although duplicating some of the point Coulomb results already contained in the literature, was required for the μ^+ calculations, for which no results were available. For the sake of completeness, the positive point Coulomb results for $f^e(\theta)$ and $g^e(\theta)$ are reproduced in Tables VI to VIII.

The whole program was checked by the following comparisons with published results. The phase shifts given in reference 11, Table I, calculated for gold, uniform charge distribution, were reproduced with good accuracy. For this purpose the rest mass of the muon was replaced by that of the electron, and t of Eq. (1c) was taken equal to 0.3×10^{-13} cm. It is interesting to note that η_1 differed from η_{-1} by about 0.03%, Yennie's value lying close by. Next, the results of reference 3 were obtained for $Z=80$, $\beta=0.2$, and also some of the point results of reference 4 were obtained. The agreement is excellent. For the μ^+ scattering the following comparisons were made: The point cross section for $\beta=0.4$, $Z=92$, agrees with that of Doggett and Spencer,¹³ and the point polarizations for $Z=80$, $\beta=0.8$ agree with those of Brown, Elton, and Mandl¹⁴ and Massey.¹⁵ The scattering of 20-Mev positrons on the extended nucleus of gold obtained by Elton and Parker¹⁶ was also reproduced.

CONCLUSIONS

For μ^- scattering on the Coulomb field of extended nuclei, the polarization² $S(\theta)$ peaks in the backward direction (Fig. 1), increases slowly with energy, and is less sensitive to the detailed shape of the charge distribution than is the cross section (Fig. 6). The cross section $\sigma(\theta)$ is quite different from the Born approximation result (Fig. 3). The product $S(\theta) \times \sigma(\theta)$ decreases rapidly with increasing energy, making the polarization measurements more favorable at lower energy (Fig. 5).

The polarization for μ^+ scattering is much smaller than that for μ^- , but strongly increases with energy (Fig. 2). For the energy region in which classical penetration into the nucleus begins to occur, the polarization changes sign with scattering angle contrary to the point-nucleus result. However in this energy region the polarization is not sensitive to the detailed shape of the nuclear charge distribution. For example, the values of both σ and S for $Z=92$, $\beta=0.6$, uniform, do not differ from the corresponding "Fermi shape" values by more than 1%. In this case the closest distance of approach for $\theta=90^\circ$ is equal to 8.4×10^{-13} cm = $1.2 \times (238)^{\frac{1}{3}} \times 10^{-13}$ cm. For larger energies the sensitivity of the polarization to the nuclear shape becomes more pronounced, as shown in Fig. 7 for the case of $Z=80$, $\beta=0.8$. Here for

TABLE VIII. μ^+ ; $\beta=0.8$; $Z=48, 80$; point. Same as Table VI for positive mesons of 70.47 Mev kinetic energy.

θ		$Z=48$	$Z=80$
30°	Re f	-2.89	-0.240
	Im f	-3.10	-7.04
	Re g	-0.256	5.78×10^{-3}
	Im g	-0.294	-0.621
	100 S_0	0.633	0.759
	σ_0	18.1	50.0
45°	Re f	-1.62	-1.59
	Im f	-0.909	-2.64
	Re g	-0.201	-0.168
	Im g	-0.127	-0.330
	100 S_0	1.38	1.64
	σ_0	3.50	9.64
60°	Re f	-0.990	-1.33
	Im f	-0.311	-1.10
	Re g	-0.151	-0.174
	Im g	-6.05×10^{-2}	-0.176
	100 S_0	2.38	2.77
	σ_0	1.10	3.04
75°	Re f	-0.658	-1.00
	Im f	-0.101	-0.482
	Re g	-0.113	-0.147
	Im g	-2.96×10^{-2}	-9.59×10^{-2}
	100 S_0	3.50	3.99
	σ_0	0.457	1.27
90°	Re f	-0.469	-0.761
	Im f	-1.71×10^{-2}	-0.206
	Re g	-8.58×10^{-2}	-0.116
	Im g	-1.42×10^{-2}	-5.28×10^{-2}
	100 S_0	4.58	5.11
	σ_0	0.227	0.638
105°	Re f	-0.354	-0.597
	Im f	1.94×10^{-2}	-7.26×10^{-2}
	Re g	-6.46×10^{-2}	-8.93×10^{-2}
	Im g	-6.38×10^{-3}	-2.92×10^{-2}
	100 S_0	5.41	5.90
	σ_0	0.130	0.370
120°	Re f	-0.282	-0.486
	Im f	3.59×10^{-2}	-5.28×10^{-3}
	Re g	-4.78×10^{-2}	-6.64×10^{-2}
	Im g	-2.41×10^{-3}	-1.59×10^{-2}
	100 S_0	5.76	6.13
	σ_0	8.32×10^{-2}	0.241
135°	Re f	-0.237	-0.414
	Im f	4.34×10^{-2}	$+2.98 \times 10^{-2}$
	Re g	-3.38×10^{-2}	-4.70×10^{-2}
	Im g	-5.57×10^{-4}	-8.46×10^{-3}
	100 S_0	5.42	5.63
	σ_0	5.90×10^{-2}	0.174
150°	Re f	-0.208	-0.368
	Im f	4.67×10^{-2}	4.81×10^{-2}
	Re g	-2.16×10^{-2}	-3.00×10^{-2}
	Im g	1.32×10^{-4}	-4.24×10^{-3}
	100 S_0	4.26	4.34
	σ_0	4.61×10^{-2}	0.139
165°	Re f	-0.193	-0.342
	Im f	4.81×10^{-2}	5.69×10^{-2}
	Re g	-1.05×10^{-2}	-1.46×10^{-2}
	Im g	2.11×10^{-4}	-1.75×10^{-3}
	100 S_0	2.35	+2.37
	σ_0	3.97×10^{-2}	0.120

$\theta=90^\circ$ the closest distance of approach is 4.1×10^{-13} cm = $0.7 \times (200)^{\frac{1}{3}} \times 10^{-13}$ cm.

¹³ J. A. Doggett and L. V. Spencer, Phys. Rev. **103**, 1597 (1956).

¹⁴ G. E. Brown, L. R. B. Elton, and F. Mandl (private communication). Their original preprint contains an error. Our agreement in the polarization for the extended nucleus $Z=80$, $\beta=0.8$ is reasonably good. The difference may well be due to the difference in nuclear shape.

¹⁵ H. S. W. Massey, Proc. Roy. Soc. (London) **A181**, 14.

¹⁶ L. R. B. Elton and K. Parker, Proc. Phys. Soc. (London) **A66**, 428 (1953).

The ratio of the cross section to the point-nucleus cross section plotted as a function of momentum transfer is shown in Figs. 3 and 4. As v/c increases, the curves appear to approach a limit which is independent of the incident momentum. This, if true, could be very valuable in extrapolating the cross section to high energies.

ACKNOWLEDGMENTS

The author wishes to thank Professor Marshak for suggesting this calculation and for providing the necessary funds for the use of the IBM 650 machine at the University's Computing Center. Acknowledgment is due to Mr. Gibson and Mr. Emmons, who valiantly carried the bulk of the programming load, thus deserving great appreciation. The author also wishes to thank Professor George Salzman for helpful discussions at the early stages of this work, and Professor Goebel for valuable criticism of the manuscript.

APPENDIX

The notation adopted is the following:

- E = total energy/ mc^2 ;
- p = momentum/ mc ;
- $\alpha = \epsilon Ze^2/\hbar c$;
- $\epsilon = +1$ for negatively charged mesons;
- $\epsilon = -1$ for positively charged mesons;
- $v/c = \beta = p/E$;
- $\gamma = \alpha/\beta$;
- $\gamma' = \gamma(1-\beta^2)^{1/2}$;
- $s_k = +(k^2-\alpha^2)^{1/2}$ for the regular solutions, denoted by superscript R ;
- $s_k = -(k^2-\alpha^2)^{1/2}$ for the irregular solutions, denoted by superscript I ;
- $\kappa = mcp/\hbar$;
- r = radial distance from the center of the nucleus;
- $x = r\kappa$, $x_0 = r_0\kappa$, where r_0 is the matching radius;
- $mc^2 = 105.7$ Mev;
- k = angular momentum quantum number $= \pm 1, \pm 2, \dots$

The radial wave functions $F_k(k)$ and $G_k(x)$,

$$G_k = r^{-1}(E-1)^{1/2}\mathcal{G}_k, \quad F_k = r^{-1}(E+1)^{1/2}\mathcal{F}_k, \quad (1A)$$

obey the radial equations

$$(d/dx - k/x)\mathcal{G}_k + (1-v_1)\mathcal{F}_k = 0, \quad (2A)$$

$$(d/dx + k/x)\mathcal{F}_k - (1-v_2)\mathcal{G}_k = 0,$$

where

$$v_1 = \Phi(E-1)/p^2, \quad v_2 = \Phi(E+1)/p^2, \quad (3A)$$

and where Φ is the Coulomb potential energy in units of mc^2 . For the example of a point nucleus, $\Phi/p = -\alpha/x$.

The phase shifts η_k are defined in the usual manner⁸ by the asymptotic form of the radial wave functions of Eq. (1A):

$$\begin{aligned} G_k &\approx r^{-1} \sin[x - (k-1)\pi/2 + \eta_k], & k > 0, \\ &\approx r^{-1} \sin[x - |k|\pi/2 + \eta_k], & k < 0. \end{aligned} \quad (4A)$$

The value of η_k is obtained in terms of the regular and irregular Coulomb phase shifts η_k^R, η_k^I and the matching coefficients $(D/C)_k$ from

$$\tan \eta_k = \frac{\sin \eta_k^R + (D/C)_k \sin \eta_k^I}{\cos \eta_k^R + (D/C)_k \cos \eta_k^I}. \quad (5A)$$

The Coulomb phase shifts are given by

$$\eta_k^{R,I} = (X+Y)_{k^{R,I}}, \quad (6A)$$

$$\begin{aligned} X_k &= (k-1-s_k)\pi/2 - \arg \Gamma(s_k+1+i\gamma), & k > 0, \\ &= X_{|k|} + \pi/2, & k < 0. \end{aligned} \quad (7A)$$

For the sake of clarity the superscripts R and I have been omitted in the above equation. The value of the argument of Γ is calculated by means of Stirling's approximation.¹⁷ The value of Y is given in the expression below, valid for both signs of k :

$$\sin Y_k = -\epsilon k [k(k+s_k) + \gamma'(\gamma'-\gamma)]^{1/2} / |k| |k-i\gamma'| \sqrt{2}, \quad (8A)$$

$$\cos Y_k = [k(k-s_k) + \gamma'(\gamma'+\gamma)]^{1/2} / |k-i\gamma'| \sqrt{2}.$$

The matching coefficients $(D/C)_k$ are obtained in terms of the radial wave functions evaluated at x_0 :

$$\left(\frac{D}{C}\right)_k = \left[\frac{\mathcal{G}'^{R,I} - \mathcal{F}'^{R,I}(\mathcal{G}/\mathcal{F})}{(\mathcal{G}/\mathcal{F})\mathcal{F}'^{R,I} - \mathcal{G}'^{R,I}} \right]_k \left(\frac{N^R}{N^I}\right)_k x_0^{2|s_k|}. \quad (9A)$$

Here \mathcal{G} and \mathcal{F} are the solutions of Eqs. (2A) and the primed quantities are related to the point Coulomb radial waves $G^{R,I}, F^{R,I}$ by means of

$$\begin{aligned} G_k^{R,I} &= r^{-1} N_k^{R,I} x_0^{s_k} \mathcal{G}_k'^{R,I}, \\ F_k^{R,I} &= r^{-1} [(E-1)/(E+1)]^{1/2} N_k^{R,I} x_0^{s_k} \mathcal{F}_k'^{R,I}. \end{aligned} \quad (10A)$$

The \mathcal{G}' and \mathcal{F}' are given by the series expansion¹⁸

$$\mathcal{G}' = \sum a_m x_0^m, \quad (11A)$$

$$\mathcal{F}' = \sum b_m x_0^m,$$

$$a_m = [-(\gamma-\gamma')a_{m-1} - (s_k+m+k)b_{m-1}] / m(m+2s_k),$$

$$b_m = [(s_k+m-k)a_{m-1} - (\gamma+\gamma')b_{m-1}] / m(m+2s_k), \quad (12A)$$

$$a_0 = 1,$$

$$b_0 = (\gamma+\gamma')/(k+s_k).$$

In Eq. (12A) the superscripts R and I and the subscripts k have been omitted for the sake of clarity.

The normalization coefficients N are obtained by comparing the G and F of Eq. (10A) with those given in

¹⁷ E. T. Whittaker and G. N. Watson, *A Course of Modern Analysis* (Cambridge University Press, Cambridge, 1927), fourth edition, Chap. 12.

¹⁸ See reference 11, Eqs. (A15) to (A17).

TABLE IX. μ^- ; $\beta=0.6$; $Z=80$. Sample partial-wave results for negative muons of 26.42 Mev kinetic energy scattering on Hg. The various symbols are defined in the Appendix. The \mathcal{F} 's and \mathcal{G} 's were calculated at the matching radius $x_0=4.4033$.

k	η_k^R (rad)	η_k^I (rad)	η_k (rad)	\mathcal{F}_k^R	\mathcal{G}_k^R	\mathcal{F}_k^I	\mathcal{G}_k^I	$(\mathcal{G}/\mathcal{F})_k$
1	3.849	2.665	2.550	-0.04499	0.08771	88.60	12.74	0.2413
-1	6.329	5.146	5.628	-0.2800	-0.6018	-9.576	9.222	-2.559
2	2.811	2.263	2.443	-0.02653	-0.04178	2.359	744.6	4.538
-2	5.582	5.033	5.434	0.8923	-0.1760	-37.81	-14.58	-0.06756
3	2.300	1.939	2.223	0.04253	-0.00393	-2208	-507.4	-0.01209
-3	5.187	4.826	5.165	-0.2017	1.235	35.68	-68.58	-5.314
4	1.962	1.692	1.952	0.08429	0.06561	-2446	-2386	0.7849
-4	4.911	4.641	4.909	-3.216	2.804	70.34	-48.69	-0.8704
5	1.711	1.495	1.710	0.1076	0.1371	-858.4	-1568	1.275
-5	4.727	4.482	4.698	-7.669	4.301	33.33	-12.03	-0.5606

TABLE X. μ^+ ; $\beta=0.6$; $Z=80$. Same as Table IX for positive muons. The \mathcal{F} 's and \mathcal{G} 's were calculated at the matching radius $x_0=4.4033$

k	η_k^R (rad)	η_k^I (rad)	η_k (rad)	\mathcal{F}_k^R	\mathcal{G}_k^R	\mathcal{F}_k^I	\mathcal{G}_k^I	$(\mathcal{G}/\mathcal{F})_k$
1	6.166	6.169	6.351	1.823	2.165	-1311	-1553	0.9059
-1	0.545	0.547	0.580	3.965	-18.64	-62.37	295.37	-0.5369
2	6.887	6.888	6.912	0.6150	1.130	-11065	-20297	1.778
-2	0.075	0.977	0.979	15.25	-18.06	811.0	961.7	-1.190
3	7.305	7.306	7.308	0.3839	1.010	-15433	-40541	2.6150
-3	1.277	1.277	1.276	25.84	-18.33	-1206.7	857.1	-0.7099
4	7.597	7.598	7.598	0.2848	0.9794	-8857	-30317	3.433
-4	1.507	1.507	1.506	36.30	-18.64	-702.6	362.6	-0.5146
5	7.822	7.822	7.822	0.2286	0.9693	-2808	-11684	4.238
-5	1.693	1.694	1.693	46.55	-18.92	-220.3	90.62	-0.4064

terms of the hypergeometric functions,⁸

$$N_k^{R,I} = -\epsilon \frac{k}{|k|} 2^{s_k} e^{\pi\gamma/2} \left[\frac{k(k+s_k) + \gamma'(\gamma' - \gamma)^{-\frac{1}{2}}}{2(k^2 + \gamma'^2)} \right]^{\frac{1}{2}} \times |\Gamma(s_k + 1 + i\gamma)| / \Gamma(2s_k + 1). \quad (13A)$$

The ratio $(N^R/N^I)_k$ is most convenient in the form

$$\left(\frac{N^R}{N^I} \right)_k = \frac{|\Gamma(\rho_k + i\gamma)|^2 (\rho_k^2 + \gamma'^2)^{\frac{1}{2}}}{|\Gamma(2\rho_k)|^2 2\rho_k} \times \frac{\cosh^2(\pi\gamma) - \cos^2\pi\rho_k}{\sin 2\pi\rho_k} \times 2^{2\rho_k} \frac{[k(k+\rho_k) + \gamma'(\gamma' - \gamma)]}{[k(k-\rho_k) + \gamma'(\gamma' - \gamma)]^{\frac{1}{2}}}; \quad (14A)$$

$$\rho_k = |s_k|.$$

Finally, the scattering amplitudes⁸ $f(\theta)$ and $g(\theta)$, from which the unpolarized cross section $\sigma(\theta)$ and polarization² $S(\theta)$ are obtained, are given in terms of the Legendre polynomials $P_k(\cos\theta)$ as

$$f(\theta) = (2i\kappa)^{-1} \sum_k c_k P_k, \quad (15A)$$

$$g(\theta) = (2i\kappa \sin\theta)^{-1} \sum_k d_k P_k,$$

$$c_k = (2k+1)[e^{2i\eta_{k+1}} - 1] + k\alpha_k,$$

$$d_k = (k+1)(k+2)\alpha_{k+1}/(2k+3) - k(k-1)\alpha_{k-1}/(2k-1), \quad (16A)$$

$$\alpha_k = e^{2i\eta_{-|k|}} - e^{2i\eta_{k+1}},$$

$$\sigma(\theta) = |f(\theta)|^2 + |g(\theta)|^2, \quad (17A)$$

$$S(\theta) = i(fg^* - gf^*) / (|f|^2 + |g|^2).$$

The connection between the right and left scattering asymmetry, the polarization of the incident beam, and the function $S(\theta)$ is the same as in reference 3, Eqs. (5) to (8).

The sums (15A) were performed by using the third-order reduced coefficients, following the method found satisfactory in reference 11, Eqs. (47) to (49), and the integration of Eq. (2A) was done by the method of the same reference, Eq. (A26).

The power series expansion (11A) becomes unreliable if x_0 is too large. The reliability limit x_M , which depends on the numerical accuracy of the computer, was estimated by means of the expression

$$\frac{\sum |a_m x_0^m| + \sum |b_m x_0^m|}{|\sum a_m x_0^m| + |\sum b_m x_0^m|} \times 10^{-7}, \quad (18A)$$

for an upper limit to the error. The factor 10^{-7} comes from assuming the numerical accuracy of each term of the sums to be good to one part in 10^{-7} .

For future reference, detailed information concerning the sample calculation for $Z=80$, $\beta=0.6$ is reproduced in Tables IX and X.